TICAM REPORT 98-01
January, 1998

A-posteriori Error Estimation for Finite Element and Generalized Finite Element Method

I. Babuska, T. Strouboulis, K. Copps,
S. K. Gangaraj and C. Upadhyay

A-posteriori Error Estimation for Finite Element and Generalized Finite Element Method

I. Babuška*

Texas Institute for Computational and Applied Mathematics,

The University of Texas at Austin, Austin, TX 78712, U.S.A.

T. Strouboulis†, K. Copps†, S.K. Gangaraj† and C. Upadhyay

Department of Aerospace Engineering, Texas A&M University,

College Station, TX 77843-3141, U.S.A.

November 24, 1997

*The work of this author was supported by the U.S. Office of Naval Research under Grants N00014-90-J-1030 and N00014-96-10019, and by the National Science Foundation under Grants DMS-91-20877 and DMS-95-01841.

†The work of these authors was supported by the U.S. Army Research Office under Grant DAAL03-G-028, by the National Science Foundation under Grant MSS-9025110, by the Texas Advanced Research Program under Grant TARP-71071, and by the U.S. Office of Naval Research under Grant N00014-96-1-0021 and Grant N00014-96-1-1015.

Abstract

In this paper we summarize our recent experiences in a posteriori error estimation for the finite element solutions of elliptic problems. In particular, we will focus on the generalized finite element method in which the character of the exact solution (for example, harmonic solutions) is taken into account in the construction of the basis functions for the finite element method. We also report the recent progress in the computer-based approach for checking the robustness of the error indicators for the energy norm of the finite element solutions in the interior of the mesh, at the boundary and in the vicinity of the corner points. In the concluding parts of the paper we give an example for the a posteriori estimation of the lower and upper bounds of the energy norm of the error and also a linear functional which represents the quantity of interest.

1 The generalized finite element method

Let us consider the model problem for solving Laplace's equation on a polygonal domain $\Omega \subset \mathbb{R}^2$ with the boundary Γ. We assume that Γ is a polygon with vertices A_i, $i = 1, \ldots, n$, as shown in Fig. 1.1. We let $\Gamma_i = \overline{A_i A_{i+1}}$, $A_{n+1} = A_1$, $i = 1, \ldots, n$, $\Gamma = \bigcup \Gamma_i$,

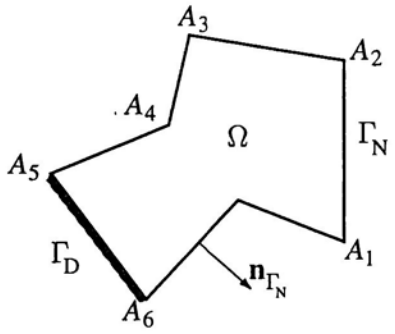

Fig. 1.1. The domain Ω.

and denote by γ_i the internal angle at A_i. We allow $\gamma_i = 2\pi$, i.e., we consider also the cracked domain. Let us be interested in solving the problem

$$-\Delta u = 0 \qquad \text{on} \quad \Omega, \tag{1.1a}$$

$$u = 0 \qquad \text{on} \quad \Gamma_D, \tag{1.1b}$$

$$\frac{\partial u}{\partial n} = g \qquad \text{on} \quad \Gamma_N \tag{1.1c}$$

where Γ_D resp. Γ_N is the Dirichlet resp. Neumann part of Γ. Denote $H^1_D = \left\{ u \in H^1(\Omega), \;\; u = 0 \text{ on } \Gamma_D \right\}$. Then the weak (exact) solution $u_0 \in H^1_D$ of the problem (1.1) satisfies

$$\int \nabla u_0 \cdot \nabla v = \int_{\Gamma_N} g\, v \qquad \forall\, v \in H^1_D\,. \tag{1.2}$$

Note that u_0 is a *harmonic* function which is singular in the neighborhoods of the vertices A_i. For simplicity we will first assume that $\Gamma_D = \emptyset$, $\Gamma = \Gamma_N$ and $\oint_\Gamma g = 0$. Let Δ be the usual finite element partition into the triangular elements τ with the nodes N_j. The patch of elements having a vertex in N_j will be denoted by ω_j.

The usual finite element solution $u_{S^p_\Delta} \in S^p_\Delta$ satisfies (1.2) for all $v \in S^p_\Delta$ where

$$S^p_\Delta = \left\{ u \in H^1(\Omega) \;\Big|\; u|_\tau \in \mathcal{P}^p(\tau), \;\; \tau \in \Delta \right\} \tag{1.3}$$

and $\mathcal{P}^p(\tau)$ is the set of all polynomials of degree p on τ. Then we have for $s \geq 1$

$$||u_0 - u_{S^p_\Delta}||_{\mathcal{U}} \leq \inf_{\chi \in u_{S^p_\Delta}} ||u_0 - \chi||_{\mathcal{U}} \leq \mathcal{C}\, h^\mu\, ||u_0||_{H^s(\Omega)} \tag{1.4}$$

where $\mu = \min(p, s-1)$, h is maximum size of the elements in Δ, $H^s(\Omega)$ is the usual Sobolev space and $||u||_{\mathcal{U}} = |u|_{H^1} = \sqrt{\int_\Omega |\nabla u|^2}$ is the energy norm.

Let us now define the *generalized FEM*. To this end, let φ_i be the usual piecewise linear "hat" function associated with the node N_i. Obviously $\sup \varphi_i \subset \omega_i$ and

$$\sum_i \varphi_i = 1$$

i.e., $\{\varphi_i\}$ is a *partition of unity*. Let us now define for $p \geq 1$

$$\hat{S}^p_\Delta = \left\{ u \;\middle|\; u = \sum_{i,j} \varphi_i\, \psi_i^{(j)} \right\} \tag{1.5}$$

where $\psi_i^{(j)}$ is the set of polynomials of degree $p-1$ on ω_i.

Theorem 1.1. We have

$$S^{p-1}_\Delta \subset \hat{S}^p_\Delta \subset S^p_\Delta \tag{1.6}$$

□

Note that (1.6) does not mean that $\{\varphi_i\, \psi_i^{(j)}\}$ is the basis of $\hat{S}^p_\Delta$. In fact, functions $\{\varphi_i\, \psi_i^{(j)}\}$ are, in general, not linearly independent. Nevertheless, as in the case of the classical finite element there exists unique (up to a constant) solution $u_{\hat{S}^p_\Delta}$, although the solution of the system of linear equations with stiffness matrix and load vector is obviously not unique. Hence, use of $\hat{S}^p_\Delta$ is essentially equivalent to the classical finite element method.

Let us now define

$$S_\Delta(\Psi) = \left\{ u \;\middle|\; u = \sum_{i,j} \varphi_i\, \psi_i^{(j)} \;\; , \psi_i^{(j)} \in \Psi_i \;\; , 1 \in \Psi_i \;\; , \Psi = \{\Psi_i\} \right\}$$

where $\psi_i^{(j)} \subset H^1(\omega_i)$ is a set of functions defined on the patch ω_i. The space Ψ_i will be called the *patch space*. Now we have:

Theorem 1.2. Assume that for all i there exists $\eta_i \in \Psi_i$ such that

$$\sum_i ||u_0 - \eta_i||^2_{\mathcal{U}(\omega_i)} \leq \mathcal{C}^2\, \varepsilon^2 \tag{1.7}$$

Then

$$||u_0 - \sum_i \varphi_i \eta_i||_{\mathcal{U}(\Omega)} \leq \mathcal{C}\, \varepsilon \tag{1.8}$$

Here $\mathcal{C}$ is a general constant which is independent of ε, u_0, Δ and Ψ, but depends on the minimal angle of the triangles $\tau \in \Delta$.

This theorem was first proven in [1], then elaborated on in [2, 3, 4, 5]. Note that η_i are defined only patch by patch and η_i are not zero on the boundaries of ω_i. Let $\Psi_i = \mathcal{P}^{p-1}(\tau_i)$ then obviously we have

$$\varepsilon \leq \mathcal{C}\, h^{\hat{\mu}}\, ||u_0||_{H^s(\Omega)} \tag{1.9}$$

where $\hat{\mu} = \min(p-1, s)$. Hence, using directly Theorem 1.2, we get a (suboptimal) error estimate. Let us now utilize the fact that u_0 *is a harmonic function.* Then it is natural to use Ψ_i as the patch space the space of harmonic polynomials of degree $p-1$ instead of the space of all polynomials. Then it can be shown (see [4]) that (1.9) holds. By a finer analysis we can prove that the rate of convergence is μ (not only $\hat{\mu}$).

Example 1.1. Let $\Omega = (-1,1) \times (-1,1)$ be a unit square and let g in (1.1c) is such that

$$u_0 = \sin x \ \sinh y \tag{1.10}$$

Assume a uniform square mesh on Ω with n^2 squares and let φ_i be the usual bilinear "hat" functions (Theorem 1.2 holds in this case too). In Fig. 1.2 we show the global relative error in the energy norm for the generalized FE method with the patch space composed by the harmonic polynomials of degree 2 and the error of usual FEM with tensor product elements of degree 3 as function of degrees of freedom N. Both methods have the same asymptotic rate of convergence $O(N^{-3/2})$. We see that in our case the generalized FE method is more effecient because it uses a smaller number of DOF by using the a-priori known information about the exact solution, namely, that u_0 is harmonic.

As we mentioned above, the generalized finite element method leads to a singular stiffness matrix. In Table 1.1 we show the nullity (rank deficiency) of the stiffness matrix of the generalized FEM when using the patch space Ψ_i composed by harmonic polynomials of degree p. The table shows that the nullity relatively decreases with n and for very small n the nullity is relatively large. This expains the lower effectivity of the generalized method and the curvature of the curve in Fig. 1.2. The generalized method is very flexible. We can combine the special shape functions with the standard FEM as

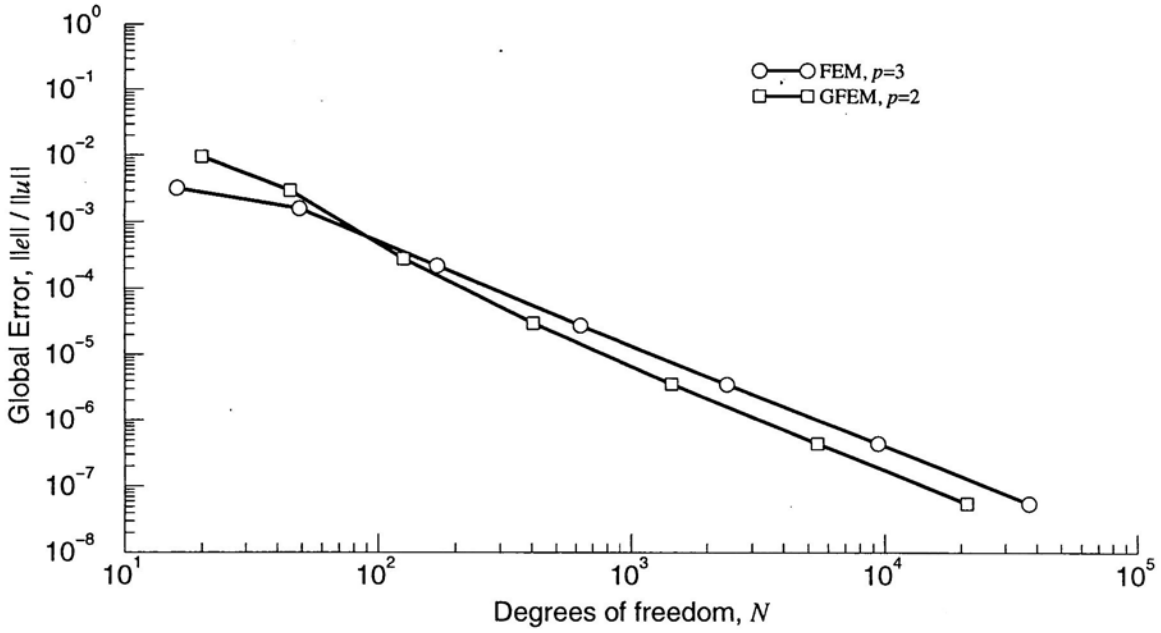

Fig. 1.2. The accuracy of the generalized FEM with patch space composed by harmonic functions of degree 2 and the standard FEM method using tensor-product elements as a function of degree of freedom. Observe the higher efficiency of the generalized FEM.

Table 1.1. The nullity of the stiffness matrix of the generalized FEM for the patch space of harmonic polynomials of degree p and number of elements n.

Elements n^2	Vertices $(n+1)^2$	Nullity / Total Degrees of Freedom				
		$p=1$	$p=2$	$p=3$	$p=4$	$p=5$
1	4	5 / 12	9 / 20	12 / 28	14 / 36	16 / 44
4	9	7 / 27	13 / 45	16 / 63	18 / 81	20 / 99
16	25	11 / 75	21 / 125	24 / 175	26 / 225	28 / 275
64	81	19 / 243	37 / 405	40 / 567	42 / 729	44 / 891
256	289	35 / 867	69 / 1445	72 / 2023	74 / 2601	76 / 28611
1024	1089	67 / 3267	133 / 5445	136 / 7623	138 / 9801	140 / 11979
4096	4225	131 / 12675	261 / 21125	264 / 29575	266 / 38025	268 / 46475
16384	16641	259 / 49923	517 / 83205	520 / 116487	522 / 149769	524 / 183051

augmentation (enrichment). Also we can use the standard FE method in the boundary elements to impose easily the essential boundary condition. We show this feature in the following example:

Example 1.2. Let Ω be the L-shaped domain shown in Fig. 1.3 with the uniform mesh of square elements. We will prescribe on $\overline{A_1 A_2}$ homogeneous Dirichlet condition and on

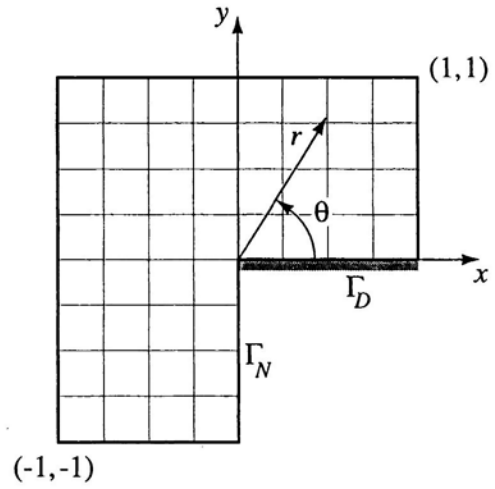

Fig. 1.3. The L-shaped domain with the square mesh of elements. (r, θ) are polar coordinates with the center at the origin.

$\overline{A_6 A_1}$ the Neumann boundary condition, so that the solution is

$$u_0 = r^{1/3} \sin \frac{1}{3} \theta \tag{1.11}$$

We will use the meshes with the size of elements $h = 1/2,\ 1/4,\ 1/8,\ldots$ and the standard FEM with tensor-product elements of degree p. Then the rate of convergence in the (relative) energy norm is $O(N^{-1/6})$ for the h version and $O(N^{-1/3})$ for the p-version. The error is shown in Fig. 1.4. In Fig. 1.4 we show also the error of the h and p versions when the space of FEM is augmented by the function

$$\Psi_1 = \left(r^{1/3} \sin \frac{1}{3} \theta\right) \varphi_1 \tag{1.12}$$

where φ_1 is the "hat" function associated with vertex A_1 and the used mesh. We see a large increase of the accuracy. Note that the rate of the augmented h-method is the same as that of the standard method, namely, $O(N^{-1/6})$ but the constant is different. This is the effect of small approximability of the exact solution by polynomials outside the singular elements. The Fig. clearly shows the effect of the augmentation by the properly

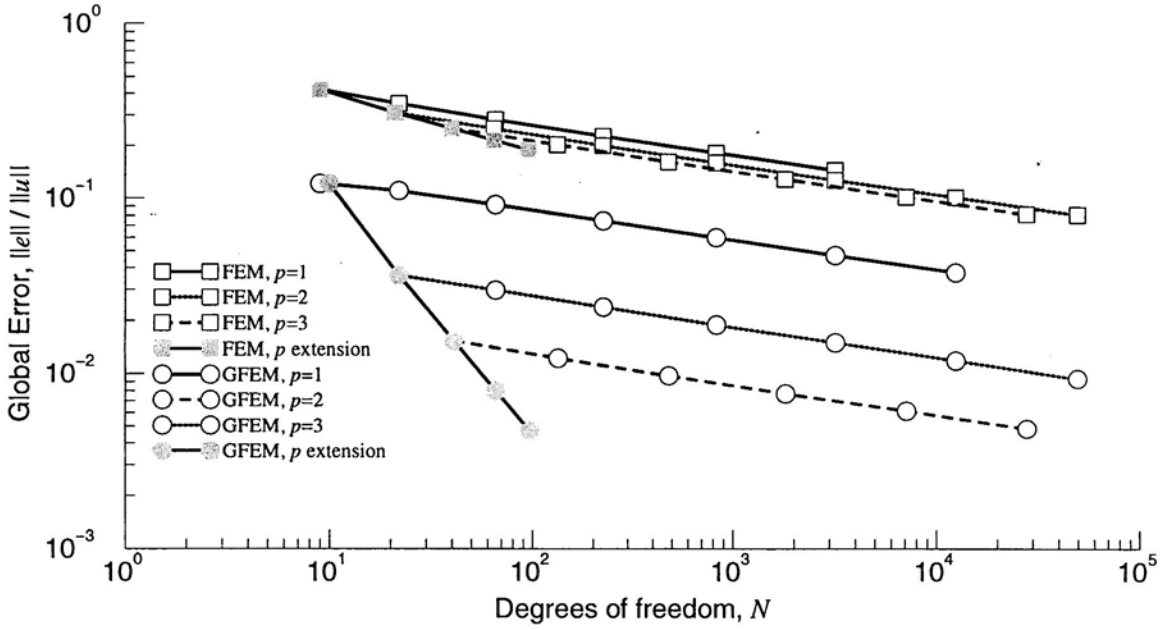

Fig. 1.4. The accuracy of the finite element solution and the generalized FEM using one additional shape function. Note the large effect of this augmentation.

selected shape function. We could of course make augmentation by two functions in the patch space Ψ_1 and also to use only harmonic polynomials in other places. Note that we had Dirichlet boundary condition on $\overline{A_1 A_2}$ and our special shape function satisfied this condition.

Let us make now additional comments about the generalized FEM as described above.

a) We can use different polynomial patch spaces in different patches. This leads naturally to the constructions of the transition elements.

b) The essential boundary conditions of Dirichlet type, homogeneous or nonhomogeneous can be implemented by the use of the usual finite element shape functions in the boundary elements.

c) The used mesh can be curvilinear.

d) The patch spaces can be constructed analytically as in the case of harmonic polynomials or Helmholtz equations (see [3]) or numerically by solving small problems. This can be used, e.g., in the case of heterogeneous materials which leads then to some kind of homogenization.

e) The generalized FEM can produce the exponential rate of convergence similarly as

in the *hp* version also in the case of problem of heterogeneous materials.

Essential part resp. difficulty of the generalized FEM is the problem of solving equations with singular positively semidefinite matrices. In the standard FE the rigid body motion leads also to the singularity of the matrix. This singularity is then avoided by fixing the displacement in a few points. Here of course the knowledge of the eigenfunctions (rigid body motion) associated to the zero eigenvalue is utilized. In the geralized FE the eigenfunctions associated with the zero eigenvalues are not known in general. Hence, let us be interested in solving the system of linear equations

$$\mathbf{A}\,\mathbf{c} = \mathbf{b} \tag{1.13}$$

stemming from the generalized FEM. Note that the solution of (1.13) exists, although it is not unique. Given the solution of (1.13) we define $u_{S^p_\Delta(\psi)}(c)$ in the obvious way. Then $u_{S^p_\Delta(\psi)}(c)$ is unique. We can compute $u_{S^p_\Delta(\psi)}(c)$ resp. (1.13) in two natural ways:

Algorithm I. Let $\mathbf{A}_\varepsilon = \mathbf{A} + \varepsilon\,\mathbf{I}$, $\varepsilon > 0$, $\mathbf{I}$ be the identity matrix. Then $\mathbf{A}_\varepsilon$ is positively definite and hence nonsingular. Now we compute in sequence

$$c_0 = \mathbf{A}_\varepsilon^{-1}\,b, \qquad r_0 = b - \mathbf{A}\,c_0, \qquad z_i = \mathbf{A}_\varepsilon^{-1}\,r_i,$$

$$v_i = \mathbf{A}\,z_i \qquad r_i = r_0 - v_1 - \cdots - v_{i-1} \qquad c_i = c_0 + \sum_{j=0}^{i-1} z_j$$

until $\dfrac{|z_i\,\mathbf{A}\,z_i|}{|c_i\,\mathbf{A}\,c_i|}$ is sufficiently small. We assume that the shape functions are such that the diagonal terms of the matrix $\mathbf{A}$ are of order 1. Then, when double precision is used, we use typically $\varepsilon = 10^{-10}$ and one iteration (c_1) is sufficient.

Algorithm II. We use the elimination with pivoting for sparse positive semidefinite matrices proposed in [6] and implemented in the Harwell library [7].

Example 1.3. Assume that we use the generalized FEM with patch spaces of harmonic polynomials of degree 4 and number of elements 4096. Then (see Table 1.1) we have DOF = 38025 and nullity is 266. Assume that the exact solution is

$$u_0 = \Re(z^5/5!) + \Im(z^5/5!)$$

where $z = x_1 + i\,x_2$. Then the generalized FE will lead to the exact solution. Hence we can test the robustness of the algorithm by computing numerically the energy $c_1^{\mathrm{T}}\,\mathbf{A}\,c_1$

with various ε and compare it with the exact energy of u_0, $||u_0||^2_{\mathcal{U}} = 0.1082162574543448$ (which was computed analytically). In Table 1.2 we give the computed energy $c_1^{\mathrm{T}} \mathbf{A}\, c_1$ by Algorithm I for various ε. We see that using $\varepsilon \leq 10^{-08}$ we get the exact solution up

Table 1.2. Computed energy $c_1^{\mathrm{T}} \mathbf{A}\, c_1$ by Algorithm I.

ε	Computed energy $c_1^{\mathrm{T}} \mathbf{A}\, c_1$
10^{-06}	0.1082162574526496
10^{-07}	0.1082162574543294
10^{-08}	0.1082162574543442
10^{-09}	0.1082162574543444
10^{-10}	0.1082162574543441
10^{-11}	0.1082162574543444
10^{-12}	0.1082162574543444

to the last digit. Hence, using in practice $\varepsilon \approx 10^{-10}$ is sufficient for all cases mentioned in Table 1.1. Let us note that we have used direct elimination without pivoting and one iteration is equivalent to an additional right-hand side computation which case is negligible.

In Table 1.3 we show the values of the energy for the same problem for different number of elements computed by Algorithm II. We of course still can use one iteration

Table 1.3. Computed energy $c^{\mathrm{T}} \mathbf{A}\, c$ by Algorithm II.

Number of Elements	Degrees of Freedom, N	Nullity	$c^{\mathrm{T}} \mathbf{A}\, c$
1	36	14	0.108216574543322
4	81	18	0.108216574543450
16	225	26	0.108216574543448
64	729	42	0.108216574543457
256	2601	74	0.108216574543457
1024	9801	138	0.108216574543190
4096	38025	266	0.108216574543463

when needed as in Algorithm I.

Let us now address the question of the computation of the error in the energy norm.

Example 1.4. Let us consider the problem addressed in Example 1.1 and compute the error measured in the energy norm. The error can be computed as the square root of the difference between exact and computed energy. In the Fig. 1.5 we show the error as a function of DOF for various degrees p for the standard FE and the generalized FE. In both cases the error decreases (asymptotically) as $O(N^{-p/2})$ but for large N it does not decrease because of round off. Note that the deterioration is about the same for the

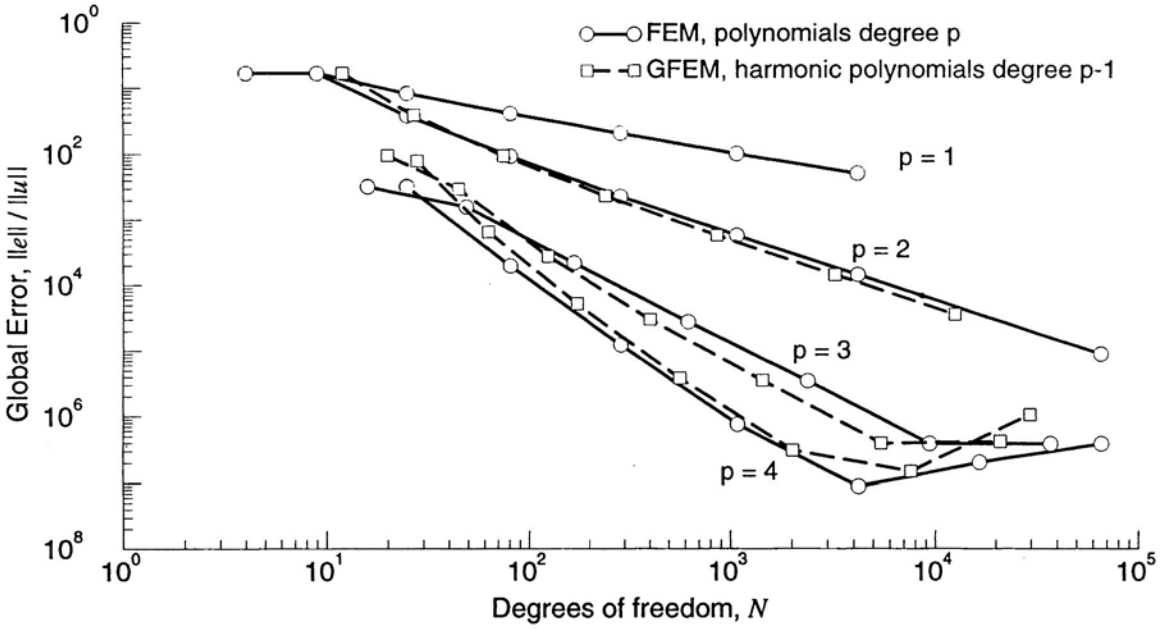

Fig. 1.5. The relative error measured in the energy norm for the solution given in (1.10) for the standard and generalized FEM computed by Algorithm II.

classical and generalized FEM. Hence, the classical FEM and the generalized FEM show the same stability with respect to the round offs.

The next problem related to generalized FEM is the problem of integration when the shape functions are singular as in the Example 1.2. There we have to integrate function having character $r^{-4/3}$, i.e., having a strong singularity. It is necessary to make the integration adaptively. There are various adaptive integration methods. One for general functions see [8] and the second is a special one aimed at the singularities of the type we are interested in [9]. In Table 1.4 we show the relative accuracy of the diagonal term k_{11} computed on the master element (i.e., for $h = 1$) as a function of the number of evaluations for various requested accuracies and the actual error when the special algorithm is used. In Fig. 1.6 we compare performance of the general algorithm and the

Table 1.4. The relative error in the integral k_{11} computed by the special algorithm for various tolerances and the actual accuracies as a function of the number of function calls.

Requested Tolerance $t_{request}$	Integrand Evaluations η_{int}	Achieved Tolerance $t_{achieved}$
0.5	147	3.53×10^{-02}
0.1	252	5.63×10^{-05}
0.05	252	5.63×10^{-05}
0.01	294	5.63×10^{-05}
0.005	399	1.16×10^{-05}
0.001	399	1.16×10^{-05}
0.0005	399	1.16×10^{-05}
0.0001	714	1.20×10^{-06}
0.00005	966	4.52×10^{-06}
0.00001	3885	3.18×10^{-06}
0.000005	4389	1.62×10^{-06}
0.000001	6237	2.35×10^{-09}
0.0000005	7749	4.64×10^{-09}
0.0000001	12201	4.02×10^{-10}

special algorithm. In Fig. 1.6 we see a very big difference in the number of function calls for the general and the special methods.

The next problem is what tolerance for the relative error should be required? This depends on the required accuracy for the finite element solution. Assume that only few elements as in the Example 1.2 have singular character. Then if relative error is of order $\eta = 1\%$, then we need to use tolerance t for integration of order $h\,\eta\,\frac{1}{100}$.

Example 1.5. Consider the problem of the Example 1.2. In the Table. 1.5 we show the error for the exact and numerical quadrature for $t = 0.25$ and $t = h/100$, when uniform h refinements are made for a $p = 1$ finite element mesh.

Above we have demonstrated the potential of the generalized FEM in the sense explained. It is very flexible and applicable to the class of meshes that are straight or curvilinear. The singular stiffness matrix does not bring any difficulties in the environment of practical accuracies. The numerical integration has to be made adaptively with the tolerance adjusted to the required accuracy. The partition of unity method resolves the problem of construction $H^1(\Omega)$ functions from the local ones, i.e., it creates conforming elements (see also [10, 11]). It is possible to use nonconforming elements with

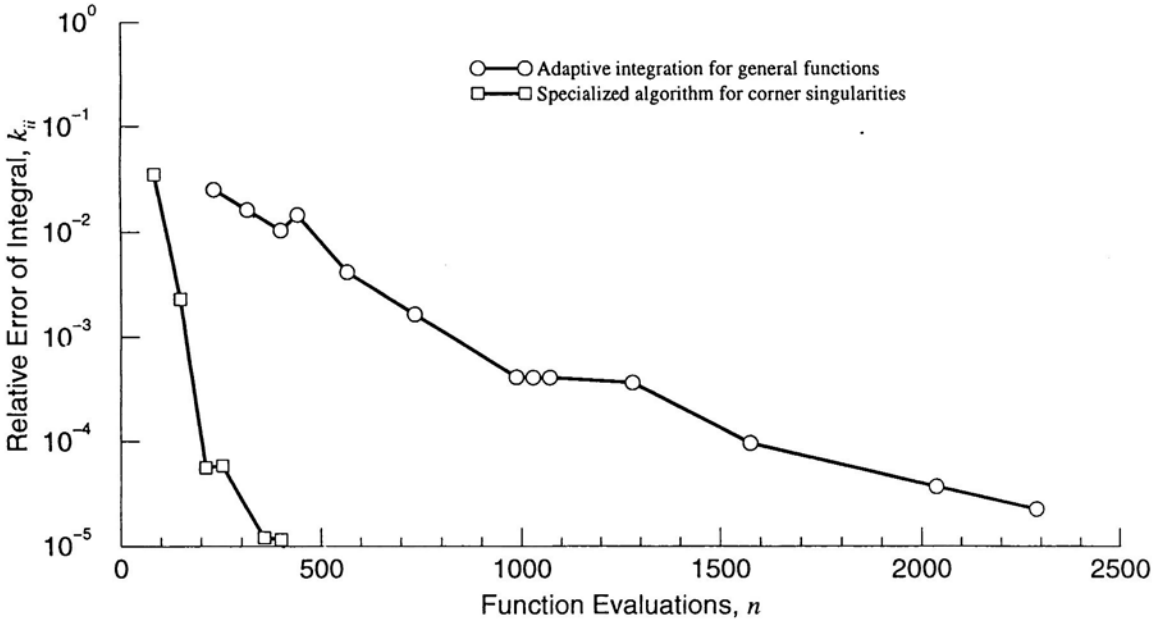

Fig. 1.6. The relative error in the integral k_{11} computed by the general algorithm for various tolerances and the actual accuracies as a function of the number of function calls.

imposing the weak conformity by different means, e.g., by a penalty method, by Lagrange multipliers, collocation, mortar approach, etc. One of the major problems here is the stability. Stability (the BB condition) can be proven in various cases; nevertheless, it is hard to analyze it in complete generality. These methods also need significant adjustment in the implementation of finite elements. Nonconforming methods can be used for various nonpolynomial shape functions, for example, satisfying the differential equation under consideration. We refer to [12], where various methods for imposing weak conformity are discussed and numerical examples are shown.

The meshless methods (see, e.g., [13]) could be interpreted as a partition of unity method too [14]. As said, the partition of unity is related to imposing the conformity of the elements. Above we used partition of unity which lead to the singular matrix. The singularity can be easily avoided by changing slighty the partition of unity function. This will lead to nonsingular matrix but the condition number could be large and this will also slightly degradate the accuracy. It will lead to the rate $h^{\bar{\mu}}$ as follows from Theorem 1.2, while as has been in Example 1.1, we can obtain accuracy $h^{\mu}(\mu = \bar{\mu} + 1)$.

We used partition of unity method with supports being patches of elements. Of course this is not needed. Circular supports of the partition of unity functions φ_i could be used. This leads to the "clouds" method [5, 10]. The disadvantage of the clouds method is the

Table 1.5.

Degrees of Freedom, N	Relative Global Error $\|\|e\|\|_{E(\Omega)}/\|\|u\|\|_{E(\Omega)}$		
	$t_{request} = 0.25$	$t_{request} = h/100$	Exact
9	0.17133036	0.17131352	0.17131350
22	0.15559454	0.15558391	0.15558390
66	0.12974370	0.12973590	0.12973590
226	0.10491205	0.10490609	0.10490609
834	0.083896447	0.083891817	0.083891817
3202	0.066801150	0.066797517	0.066797517
12546	0.053095143	0.053092279	0.053092279

expensive (integration) construction of the stiffness matrix. The same is true in general for the "meshless" method which is essentially a cloud method. Another disadvantage of the cloud method is imposing the essential boundary condition. The same problems occur for the meshless method. The main advantage of the geralized FEM as explained above is that the usual FE implementational techniques could be utilized (e.g., integration is dome on master element, etc.) and that the method is very flexible (e.g., implementation of essential (Dirichlet) boundary condition by using polynomial shape functions) and the shape functions could be constructed adaptively.

2 A-posteriori error estimation

Numerical analysis aims at computation of certain data of interest and a-posteriori estimates of the error in these computed data are needed. Various goals could be of interest. For example, in a "hot spot" area the goal is to compute maximal stresses or displacements (i.e., in our problem (1.1) fluxes resp. solution), the stress intensity factor in the corner. We are interested in the a-posteriori error estimation of these computed values or in the error of the finite element solution in the whole Ω or its part when measured in some norm, e.g., in the energy norm, etc. We will address here first the error of the finite element solution when the mesh is locally uniform consisting of repeating cells of more complicated structure and then generalize these results.

Let us consider four types of cells shown in the Fig. 2.1. These patterns have typical

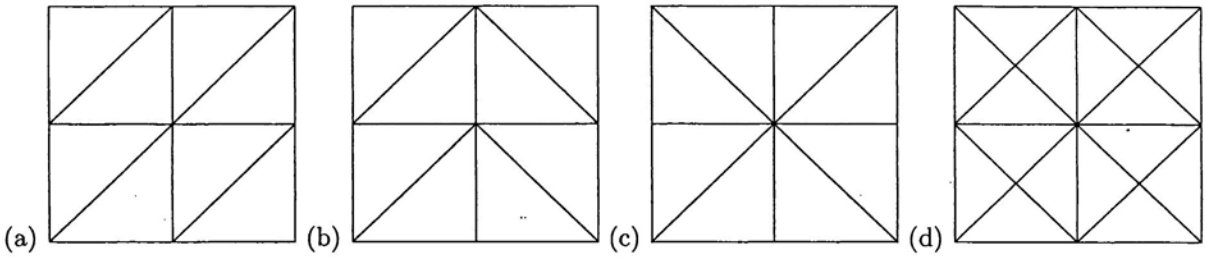

Fig. 2.1. Cells with regular pattern of elements: (a) regular, (b) chevron, (c) union jack, (d) criss cross.

topologies occurring in the mesh generators. We will assume that the cells are uniform and translation invariant in the areas of interest which are:

a) inside the domain

b) at the boundary

c) in the neighborhood of the vertex

We will analyze the a-posteriori estimation of the error of FEM using these meshes.

2.1 Analysis of the accuracy of the classical finite element solution inside the domain Ω

Let $\mathbf{x}^0 = (x_1^0, x_2^0) \in \Omega$ and define

$$S(\mathbf{x}^0, H) = \left\{ x = (x_1, x_2) \;\middle|\; |x_i - x_i^0| < H, \;\; i = 1, 2 \right\}$$

and let $\bar{S} \subset \Omega$. We will assume that the finite element mesh is uniform in $S(\mathbf{x}^0, H)$ composed by the cells of side length h and topology shown in Fig. 2.1. Outside of $S(\mathbf{x}^0, H)$ the mesh is arbitrary but is such that Assumption III, spelled out below, holds. Let u_0 be the exact solution of the problem (1.1) and u_h be the finite element solution using elements of degree p. We will assume the following:

Assumption I: On $\bar{S}(\mathbf{x}^0, H)$

$$|D^\alpha u_0| \leq K < \infty, \qquad 0 \leq |\alpha| \leq p + 2 \tag{2.1}$$

This assumption states that the exact solution u_0 is sufficiently smooth on $S(\mathbf{x}^0, H)$.

Assumption II: If $a_\alpha =_{\text{df}} (D^\alpha u)(x^0)$, $\alpha = (\alpha_1, \alpha_2)$, and $|\alpha| \leq p + 1$, then

$$R^2 = \sum_{|\alpha| = p+1} (a_\alpha)^2 > 0 \tag{2.2}$$

This assumption states that u_0 is not a polynomial of degree p.

Assumption III: Let $H_1 < H$. Then

$$||u - u_h||_{L^2(S(\mathbf{x}^0, H_1))} \leq \mathscr{C}\, h^\beta\, H_1 \tag{2.3}$$

where $\beta \geq (p+1) - \varepsilon$, $\varepsilon = \dfrac{1}{6(6p+1)}$ and $\mathscr{C}$ is independent of the mesh and H_1 but depends on K and R. This assumption states that the pollution is negligible. For example, we have to assume that in the neighborhood of the corners there is sufficient mesh refinement and hence Assumption III implicitly is an assumption about the mesh outside $S(\mathbf{x}^0, H)$. This assumption can be replaced by the assumption

$$||u_0 - u_h||_{L^\infty(S(\mathbf{x}^0, H_1))} \leq \mathscr{C}\, h^\beta$$

If the exact solution is sufficiently smooth as well as the domain, then $\beta = p+1$ for $p > 1$ (for $p = 1$, we have $h^2 \ln h$ instead of h^2). Under Assumptions I–III we have the following theorem [15]:

Theorem 2.1. Let $\mathscr{C}_1\, H_1^\alpha \leq h < \mathscr{C}_2\, H_1^\alpha$, $\alpha < 1$ and let $\nu = \dfrac{6p+1}{6p}$ and $H_1 < H$. Then for any $x \in S(\mathbf{x}^0, H_1)$ we have

$$\frac{\partial e_h}{\partial x_i}(\mathbf{x}) = \frac{\partial \psi}{\partial x_i}(\mathbf{x}) + \lambda \mathscr{C}\, h^{p+\nu}, \qquad i = 1, 2 \tag{2.4}$$

where $e_h = u_0 - u_h$, $|\lambda| \leq 1$, $\mathscr{C}$ is independent of h and function $\psi(\mathbf{x})$ is a periodic function with the period of the cell size and can be constructed by analyzing the single cell only, while

$$\sum_{i=1,2} \left\| \frac{\partial e_h}{\partial x_i} \right\|_{L^\infty(S(\mathbf{x}^0, H))} \geq \mathscr{C}\, h^p$$

□

The construction of ψ is given in [15] and depends on the differential operator of the equation under consideration. Theorem 2.1 shows that we can asymptotically, as $h \longrightarrow 0$, compute e_h by assuming that u_0 is homogeneous polynomial of degree $p+1$ (because the finite element solution reproduces the polynomial of degree p).

Theorem 2.1 assumes that there is negligible pollution as defined in Assumption III.

Nevertheless, let us elaborate on it more. The error e_h obviously satisfies

$$\begin{aligned} -\Delta e_h &= R_h \qquad \text{on} \quad \Omega \\ \frac{\partial e_h}{\partial n} &= r_h \qquad \text{on} \quad \Gamma_{\mathrm{N}} \\ e_h &= 0 \qquad \text{on} \quad \Gamma_{\mathrm{N}} \end{aligned}$$

where $R_h \in H^{-1}(\Omega)$ is the residuum which consists of two parts: one is functions from $L^2(\tau)$, the other is Dirac functions on the edges of elements; and $r_h \in H^{-1/2}(\Gamma_{\mathrm{N}})$. Let us now write $R_h = R_h^{(1)} + R_h^{(2)}$ where $R^{(2)} = 0$ in the neighborhood of the cell c under consideration. Then we can write $e_h = e_h^{(1)} + e_h^{(2)}$ and the assumption about negligible pollution is equivalent to the assumption that $||e_h^{(2)}||_{\mathcal{U}(c)} \ll ||e_h^{(1)}||_{\mathcal{U}(c)}$. Further, because function ψ in (2.4) is periodic, we see that $e_h^{(1)} \approx \psi$ reflects the effects of residuum not only in the particular cell but of the residuum in *the entire neighborhood of the cell.* This observation is essential also for the results given in [16].

Theorem 2.1 leads to the possibility to compute asymptotically the effectivity index of an elemental estimator in the energy norm $\mathcal{E}(u)$:

$$\kappa(u_0) = \frac{\mathcal{E}(u_0)}{||u_0 - u_h||} \tag{2.5}$$

on the cell or an element of the cell. In (2.5) we have to assume that the estimator $\mathcal{E}$ is a stable one (all estimators proposed in the literature are stable). For more, see [17]. The effectivity index $\kappa(u)$ defined in (2.5) depends only on u_0 being homogeneous polynomial of degree $p+1$ and is computable by analyzing one cell only. Denoting by $\hat{\mathcal{P}}^{p+1}$ the set of homogeneous polynomials of degree $p+1$ we can now compute

$$\kappa_L(\mathcal{E}, \hat{\mathcal{P}}^{p+1}) = \inf_{u \in \hat{\mathcal{P}}^{p+1}} \frac{\mathcal{E}(u)}{||e||} \tag{2.6a}$$

$$\kappa_U(\mathcal{E}, \hat{\mathcal{P}}^{p+1}) = \sup_{u \in \hat{\mathcal{P}}^{p+1}} \frac{\mathcal{E}(u)}{||e||} \tag{2.6b}$$

where κ_L and κ_U are the lowest and largest eigenvalue of certain matrices.

Now we can introduce the robustness index $\mathcal{R}$ of the estimator $\mathcal{E}$ (see, e.g., [15, 17, 18])

$$\mathcal{R}(\mathcal{E}, \hat{\mathcal{P}}^{p+1}) = \max\left(|1 - \kappa_L|, \left|1 - \frac{1}{\kappa_L}\right|, |1 - \kappa_U|, \left|1 - \frac{1}{\kappa_U}\right|\right)$$

where "ideal" robustness index has value 0. (2.6) depends obviously on the topology of the cell and the robustness index $\mathcal{R}(\mathcal{E})$ describes the (asymptotic) quality of the

estimator for the used particular topology. Hence we can take into consideration a set τ of topologies of the cells, e.g., shown in Fig. 2.1 or any other, for example, parametric set $\tau(\alpha)$, where α is the aspect ratio or skewness of the cell. Then we can define

$$\kappa_L(\mathcal{E}, \hat{\mathcal{P}}^{p+1}, \tau(\alpha)) = \inf_{\hat{\mathcal{P}}^{p+1}, \tau(\alpha)} \frac{\mathcal{E}(u_0)}{||e_h||}$$

$$\kappa_U(\mathcal{E}, \hat{\mathcal{P}}^{p+1}, \tau(\alpha)) = \sup_{\hat{\mathcal{P}}^{p+1}, \tau(\alpha)} \frac{\mathcal{E}(u_0)}{||e_h||}$$

and associated robustness index $\mathcal{R}(\mathcal{E}, \hat{\mathcal{P}}^{p+1}, \tau(\alpha))$. If we are interested only in the class of problems (1.1), then the solution is harmonic, and hence, we can restrict the set $\hat{\mathcal{P}}^{p+1}$ to the set of homogeneous harmonic polynomials $\hat{\mathcal{P}}_H^{p+1}$ and associated index $\mathcal{R}(\mathcal{E}, \hat{\mathcal{P}}_H^{p+1}, \tau(\alpha))$. Also analogously, we can consider the whole class of differential equation, e.g., of anisotropic operators, etc. [17, 18], and also other norms. Comparing different error estimators, we prefer the one with the smallest robustness index. We underline that this ranking is based on

1) asymptotic behavior, i.e., for $h \longrightarrow 0$

2) smoothness of the solution

3) negligible pollution

4) class of operators, mesh topologies, norm

For example, the performance can be different for the four topologies mentioned in Fig. 2.1 and excluding one of them can decrease the robustness index. In [17, 18] we have shown that this is indeed the case. We addressed only very regular meshes. Much more general meshes can be addressed by the periodization principle. By this we mean that a small part of a particular mesh is augmented to a periodic cell, which then can be analyzed as above. This was done in [19] and shown that the ranking of the estimators is essentially the same.

Based on this analysis the following conclusions were made:

a) The equilibrated error estimators are more robust than the unequilibrated ones.

b) The ZZ estimator is the most robust one.

For the definition of these estimators, we refer to [17]. These conclusions are reached under the following assumptions:

a) The exact solution is smooth.

b) The elements are sufficiently small.

c) The elements are not close to the boundary.

d) The elements are of degree $p = 1$ or $p = 2$.

For a detailed analysis and extensive numerical results, we refer to [17, 18]. Here we have addressed triangular and quadrilateral elements for the general anisotropic heat and elasticity equations.

We remark that Theorem 2.1 can be used for the analysis of the superconvergence effects [15].

2.2 Analysis of the accuracy of the classical finite element solution close to the boundary

Let us now address the problem of the elements at the straight boundary. The assumptions here are analogous as in the Section 2.1. In Fig. 2.2 we show typical character of the cell uniform mesh at the boundary. Analogously as in the previous case we have the

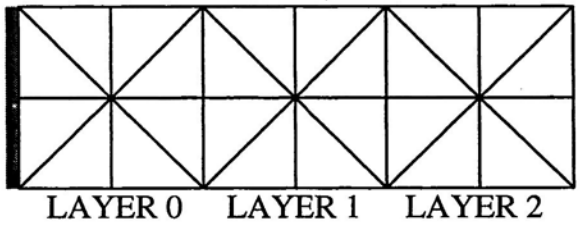

Fig. 2.2. The uniform cell mesh (union jack pattern) at the boundary.

asymptotic expression for the error.

Theorem 2.2. [20] Let the assumptions of Theorem 2.1 hold. Then

$$\frac{\partial e_h}{\partial x_i}(\mathbf{x}) = \frac{\partial \psi}{\partial x_i}(\mathbf{x}) + \frac{\partial \psi_{BL}}{\partial x_i} + \lambda \mathcal{C}\, h^{p+\nu}, \qquad i = 1, 2 \tag{2.7}$$

where ψ is the same as in the Theorem 2.1 and ψ_{BL} is the boundary layer function which is periodic in the x direction. □

The function ψ_{BL} has to be analyzed on the entire strip shown in Fig. 2.2; this is done by solving an associated eigenvalue problem. The decay of ψ_{BL} is exponential with the rate $-\lambda/h$, where $\lambda > 0$ depends on the topology of the mesh and on the differential equation. As in the Section 2.1 we can restrict ourselves to the case of exact solution being homogeneous polynomials of degree $p+1$ satisfying homogeneous boundary conditions. Analogously as in Section 2.1, we can now analyze the robustness of particular error estimators. In [20] we have shown the following:

a) The equilibrated residual estimator for the Dirichlet (essential) boundary conditions performs much worse than for the Neumann (natural) boundary conditions.

b) The ZZ estimator is the most robust one.

For detailed analysis and extensive numerical results, we refer to [20].

Let us note that in the same vein the Theorem 2.2 can be used for the analysis of superconvergent effects in the elements close to the boundary.

2.3 Analysis of the accuracy of the classical finite element solution in the neighborhood of the corners

Let us consider the problem of the accuracy in the neighborhood of the corner or the crack. For simplicity we will address here explicitly the angle 270°, although the analysis applies in general and computations were made for the general case too. Hence, we consider the cell mesh shown in Fig. 2.3. (We mention that when the angle is not 270°

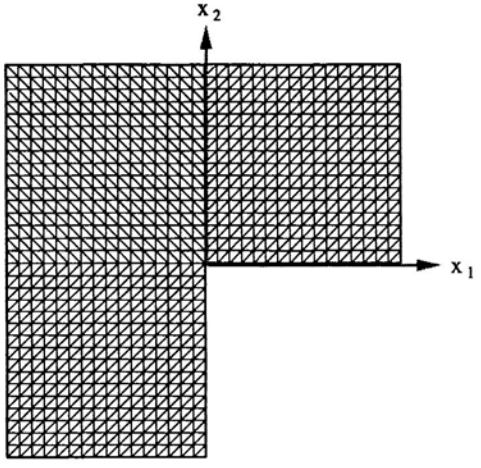

Fig. 2.3. The uniform cell mesh in the neighborhood of the corner.

we use other translation-invariant cell distributions.) Analogously as in the Section 2.1 we will consider the neighborhood of the size H_1 and size of the cells h. The exact solution u_0 in the neighborhood of the vertex has forms

$$u_0(r,\theta) = C\, r^{\alpha} \sin\alpha\,\theta + \text{ smoother terms} \tag{2.8a}$$

or

$$u_0(r,\theta) = C\, r^{\alpha} \cos\alpha\,\theta + \text{ smoother terms} \tag{2.8b}$$

where $\alpha = \pi/\omega$ or $\alpha = \pi/(2\omega)$ depending on the imposed boundary conditions, and ω is the internal angle at the vertex A_1. In (2.8) (r,θ) are the polar coordinates with the origin at the vertex. We can prove the theorem analogous to the Theorems 2.1 and 2.2.

Theorem 2.3. [21] Assume that

a) The mesh is cell uniform in the neighborhood of the vertex $A_1 = x^0 = 0$, and $\mathscr{C}_1 H_1^{\alpha} \le h \le \mathscr{C}_2 H_1^{\alpha}$, $\alpha = \alpha(p)$ is properly selected.

b) The solution u_0 has form (2.8) with $|C| > 0$.

c) The pollution is negligible, i.e.,

$$||u_0 - u_h||_{L^2(S(0,H_1)\cap\Omega)} \le \mathscr{C}\, h^{\beta}\, H_1$$

where $\beta > \min(2\alpha - \varepsilon_1, p+1-\varepsilon_2)$ and $\varepsilon_1, \varepsilon_2 > a$ are properly chosen.

d) Let $\Omega(H_1) = S(0,H_1)\cap\Omega$ and ψ_h be the finite element solution on $\Omega(H_1)$ with Neumann boundary conditions on $\partial\Omega(H_1) - \Gamma$ with exact solution $U = r^{\alpha}\sin\alpha\,\theta$ (resp. $r^{\alpha}\cos\alpha\,\theta$). Then in any $\Omega(\rho h)$, $\rho = 1,\ldots,\rho_0$, where ρ_0 is independent of h, we have with $\nu > 0$

$$\left\| \frac{\partial e_h}{\partial x_i} - \frac{\partial \psi_h}{\partial x_i} \right\|_{L^2(\Omega(\rho h))} \le \mathscr{C}\, h^{\mu+\nu}, \qquad i = 1,2 \tag{2.9}$$

where $\mu = \min(\alpha, p)$ and $\mathscr{C}$ is independent of h, while

$$\left\| \frac{\partial e_h}{\partial x_i} \right\|_{L^2(\Omega(\rho h))} \ge \mathscr{C}\, h^{\mu}, \qquad i = 1,2$$

□

Theorem 2.3 can be used for the asymptotic analysis of the a-posteriori error estimation in the energy norm analogously as before. In contrast to the previous cases, namely, of the elements inside or at the boundary, here we have to consider only one function (2.8) and not the entire set. Hence, the robustness index is related only to the topology of the mesh, the boundary conditions and the differential operator. We note that Theorem 2.3, with some modifications, can also be used for the analysis of the superconvergent effects. As an example, let us consider the case in which the cell-wise effectivity index on the cracked and L-shaped domain shown in Fig. 2.4, where the numbering of the elements is shown too. We will consider the equilibrated residual estimators $ERpB$ and the ZZ es-

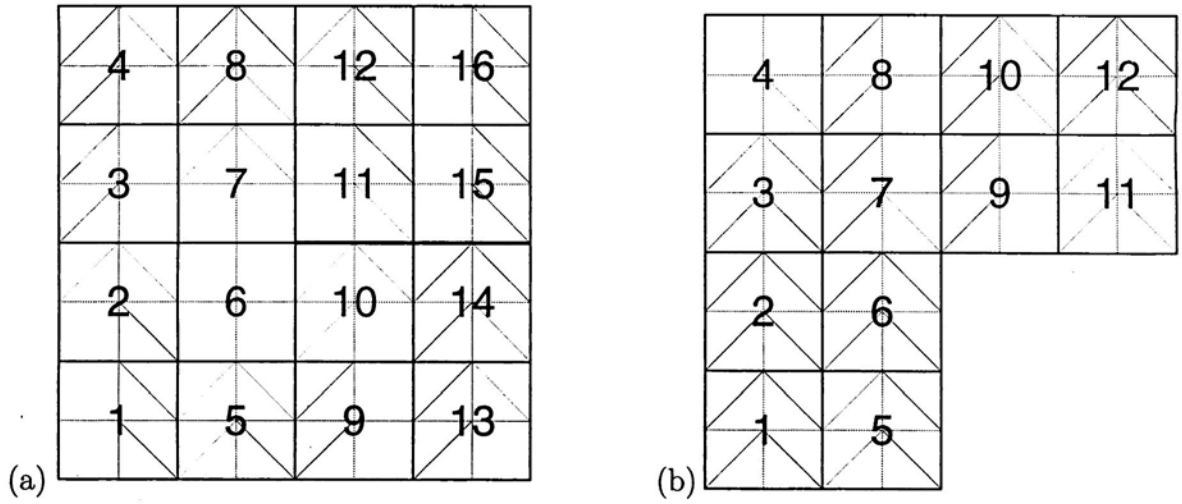

Fig. 2.4. The neighborhood of the vertex with cell enumeration. An example of enumeration of the cells for chevron pattern for: (a) The cracked domain. (b) The L-shaped domain.

timators which were most robust inside the domain and at the boundary. In Tables 2.1a and 2.1b we report the (cell) effectivity indices on the cracked domain shown in Fig. 2.4a for the homogeneous boundary conditions and exact solution with leading terms

$$u = r^{1/4} \sin \frac{\theta}{4} \tag{2.10a}$$

$$u = r^{1/2} \sin \frac{\theta}{2} \tag{2.10b}$$

of different strength of the singularity. In Tables 2.2a and 2.2b we report the (cell) effectivity indices on the L-shaped domain shown in Fig. 2.4b for the exact solution with loading terms

$$u = r^{1/3} \sin \frac{\theta}{3} \tag{2.11a}$$

Table 2.1a. The local quality of error estimators for patchwise uniform meshes on the cracked domain. Laplace equation; $u = r^{1/4}\sin(\theta/4)$; elements of order $p = 1, 2$. The cellwise effectivity index for the $ERpB$ and the ZZ estimators.

Cell No.	Regular pattern		Chevron pattern		Union Jack pattern		Criss Cross pattern	
	$ERpB$	ZZ	$ERpB$	ZZ	$ERpB$	ZZ	$ERpB$	ZZ
Linear Elements ($p = 1$)								
1	0.491	0.516	0.492	0.457	0.492	0.499	0.355	0.359
2	0.599	0.676	0.605	0.598	0.611	0.591	0.402	0.411
3	0.348	0.313	0.344	0.354	0.343	0.341	0.384	0.389
4	0.289	0.288	0.288	0.273	0.288	0.292	0.243	0.245
5	0.539	0.665	0.548	0.561	0.558	0.544	0.591	0.601
6	1.382	0.743	1.176	0.865	1.378	0.664	1.364	0.655
7	**1.545**	**0.544**	**1.869**	**0.458**	**1.869**	**0.527**	**1.862**	**0.547**
8	0.379	0.372	0.380	0.383	0.379	0.369	0.224	0.229
9	0.832	0.776	0.815	0.821	0.828	0.799	0.667	0.680
10	0.749	1.004	0.749	1.132	0.779	0.969	0.716	0.952
11	**2.064**	**0.379**	**2.056**	**0.303**	**2.059**	**0.379**	**1.925**	**0.384**
12	0.204	0.245	0.207	0.202	0.207	0.213	0.239	0.242
13	0.729	0.732	0.731	0.678	0.729	0.741	0.523	0.530
14	0.775	0.763	0.779	0.730	0.791	0.849	0.786	0.802
15	0.223	0.231	0.225	0.228	0.225	0.236	0.167	0.169
16	0.159	0.171	0.161	0.163	0.161	0.161	0.191	0.192
Quadratic Elements ($p = 2$)								
1	0.072	0.079	0.073	0.084	0.072	0.075	0.039	0.038
2	0.092	0.107	0.092	0.101	0.091	0.090	0.059	0.058
3	0.086	0.092	0.086	0.095	0.086	0.087	0.048	0.047
4	0.042	0.044	0.043	0.043	0.043	0.042	0.024	0.023
5	0.139	0.159	0.138	0.160	0.138	0.140	0.078	0.077
6	1.573	0.819	1.219	0.904	1.573	0.654	1.561	0.649
7	**1.671**	**0.572**	**2.192**	**0.499**	**2.194**	**0.534**	**2.198**	**0.557**
8	0.057	0.062	0.057	0.063	0.057	0.056	0.038	0.037
9	0.156	0.169	0.155	0.182	0.154	0.154	0.096	0.095
10	0.667	1.093	0.672	1.219	0.761	1.073	0.696	0.973
11	**2.286**	**0.399**	**2.288**	**0.306**	**2.289**	**0.427**	**2.199**	**0.419**
12	0.057	0.063	0.057	0.063	0.057	0.057	0.032	0.031
13	0.127	0.134	0.127	0.149	0.127	0.133	0.068	0.065
14	0.199	0.362	0.201	0.233	0.197	0.429	0.116	0.118
15	0.045	0.051	0.055	0.054	0.055	0.071	0.029	0.027
16	0.028	0.032	0.028	0.030	0.029	0.026	0.018	0.017

Table 2.1b. The local quality of error estimators for patchwise uniform meshes on the cracked domain. Laplace equation; $u = r^{1/2}\sin(\theta/2)$; elements of order $p = 1, 2$. The cellwise effectivity index for the $ERpB$ and the ZZ estimators.

Cell No.	Regular pattern		Chevron pattern		Union Jack pattern		Criss Cross pattern	
	$ERpB$	ZZ	$ERpB$	ZZ	$ERpB$	ZZ	$ERpB$	ZZ
Linear Elements ($p = 1$)								
1	0.879	0.912	0.881	0.823	0.879	0.888	0.791	0.798
2	0.889	1.034	0.901	0.916	0.911	0.888	0.793	0.985
3	0.919	0.853	0.911	0.900	0.911	0.888	0.973	0.985
4	0.880	0.880	0.879	0.832	0.879	0.888	0.791	0.798
5	0.943	1.014	0.946	0.922	0.954	0.929	0.842	0.857
6	1.007	1.137	0.996	1.309	1.017	1.023	0.837	1.053
7	**0.874**	**1.100**	**0.861**	**0.932**	**0.893**	**1.023**	**0.975**	**1.053**
8	0.956	0.928	0.955	0.959	0.954	0.929	0.842	0.857
9	0.695	0.655	0.686	0.696	0.688	0.698	0.827	0.834
10	1.112	0.888	1.186	1.034	1.559	0.930	1.269	0.908
11	**1.393**	**0.951**	**1.289**	**0.794**	**1.355**	**0.930**	**1.442**	**0.908**
12	0.675	0.796	0.687	0.677	0.688	0.698	0.827	0.834
13	0.631	0.618	0.627	0.617	0.628	0.628	0.733	0.737
14	0.757	0.740	0.764	0.720	0.766	0.794	0.651	0.663
15	0.760	0.784	0.766	0.769	0.766	0.794	0.651	0.663
16	0.624	0.659	0.629	0.629	0.628	0.628	0.733	0.737
Quadratic Elements ($p = 2$)								
1	0.354	0.377	0.352	0.400	0.356	0.356	0.247	0.237
2	0.485	0.553	0.492	0.531	0.480	0.477	0.347	0.338
3	0.485	0.515	0.480	0.522	0.480	0.477	0.347	0.338
4	0.354	0.375	0.357	0.365	0.356	0.356	0.247	0.237
5	0.381	0.437	0.386	0.425	0.381	0.367	0.305	0.295
6	1.049	1.300	0.965	1.423	1.053	1.061	0.811	1.079
7	**0.789**	**1.242**	**0.807**	**1.063**	**0.874**	**1.061**	**1.006**	**1.079**
8	0.379	0.413	0.381	0.412	0.381	0.367	0.305	0.295
9	0.386	0.408	0.385	0.416	0.388	0.387	0.258	0.251
10	1.003	0.975	1.056	1.176	1.689	1.076	1.409	1.036
11	**1.467**	**1.043**	**1.364**	**0.846**	**1.464**	**1.076**	**1.615**	**1.036**
12	0.387	0.427	0.392	0.419	0.388	0.387	0.258	0.251
13	0.232	0.240	0.238	0.246	0.235	0.218	0.170	0.163
14	0.321	0.422	0.309	0.358	0.342	0.469	0.233	0.222
15	0.311	0.345	0.372	0.364	0.371	0.469	0.231	0.222
16	0.233	0.259	0.230	0.248	0.235	0.218	0.170	0.163

Table 2.2a. The local quality of error estimators for patchwise uniform meshes on the L-shaped domain. Laplace equation; $u = r^{1/3}\sin(\theta/3)$; elements of order $p = 1, 2$. The cellwise effectivity index for the $ERpB$ and the ZZ estimators.

Cell No.	Regular pattern		Chevron pattern		Union Jack pattern		Criss Cross pattern	
	$ERpB$	ZZ	$ERpB$	ZZ	$ERpB$	ZZ	$ERpB$	ZZ
Linear Elements ($p = 1$)								
1	0.770	0.805	0.772	0.715	0.770	0.781	0.593	0.600
2	0.845	0.961	0.854	0.849	0.863	0.835	0.710	0.724
3	0.573	0.519	0.567	0.577	0.567	0.559	0.657	0.665
4	0.512	0.511	0.511	0.484	0.512	0.517	0.437	0.441
5	0.827	0.830	0.808	0.755	0.820	0.875	0.848	0.859
6	0.860	1.039	0.827	1.079	0.860	1.008	0.796	0.955
7	**1.243**	**0.679**	**1.467**	**0.586**	**1.467**	**0.573**	**1.455**	**0.559**
8	0.635	0.621	0.636	0.640	0.635	0.618	0.413	0.422
9	1.824	0.540	1.815	0.426	1.815	0.504	1.690	0.536
10	0.346	0.414	0.352	0.344	0.352	0.361	0.428	0.432
11	**0.387**	**0.401**	**0.390**	**0.395**	**0.390**	**0.408**	**0.299**	**0.306**
12	0.285	0.304	0.288	0.289	0.288	0.287	0.349	0.351
Quadratic Elements ($p = 2$)								
1	0.166	0.179	0.167	0.193	0.167	0.172	0.096	0.093
2	0.195	0.225	0.196	0.213	0.193	0.191	0.131	0.127
3	0.181	0.192	0.179	0.197	0.179	0.181	0.105	0.104
4	0.095	0.099	0.095	0.097	0.095	0.095	0.057	0.055
5	0.254	0.286	0.252	0.316	0.251	0.518	0.156	0.158
6	0.847	1.102	0.739	1.159	0.843	1.098	0.777	0.973
7	**1.303**	**0.751**	**1.680**	**0.653**	**1.683**	**0.539**	**1.679**	**0.534**
8	0.117	0.129	0.117	0.129	0.118	0.114	0.082	0.079
9	1.995	0.559	1.999	0.430	1.999	0.549	1.919	0.573
10	0.116	0.129	0.117	0.128	0.117	0.117	0.068	0.067
11	**0.092**	**0.103**	**0.112**	**0.109**	**0.112**	**0.144**	**0.061**	**0.058**
12	0.060	0.068	0.059	0.064	0.061	0.056	0.039	0.038

Table 2.2b. The local quality of error estimators for patchwise uniform meshes on the L-shaped domain. Laplace equation; $u = r^{2/3}\sin(2\theta/3)$; elements of order $p = 1, 2$. The cellwise effectivity index for the $ERpB$ and the ZZ estimators.

Cell No.	Regular pattern		Chevron pattern		Union Jack pattern		Criss Cross pattern	
	$ERpB$	ZZ	$ERpB$	ZZ	$ERpB$	ZZ	$ERpB$	ZZ
Linear Elements ($p = 1$)								
1	0.867	0.905	0.872	0.857	0.871	0.872	0.929	0.933
2	0.893	1.027	0.904	0.927	0.909	0.912	0.980	0.987
3	1.009	0.973	1.005	0.962	1.006	0.981	1.007	1.018
4	0.975	0.976	0.975	0.926	0.975	0.982	0.929	0.936
5	0.947	0.972	0.944	0.884	0.953	0.976	0.879	0.895
6	1.345	1.136	1.042	1.155	1.315	1.068	1.072	1.049
7	**0.893**	**1.095**	**0.889**	**0.970**	**0.883**	**0.947**	**0.801**	**0.969**
8	1.009	0.973	1.007	1.007	1.006	0.981	1.007	1.018
9	1.136	1.136	1.108	0.939	1.127	1.068	1.229	1.049
10	0.893	1.027	0.909	0.900	0.909	0.912	0.980	0.987
11	**0.946**	**0.972**	**0.953**	**0.949**	**0.953**	**0.976**	**0.880**	**0.895**
12	0.867	0.905	0.872	0.867	0.871	0.872	0.929	0.933
Quadratic Elements ($p = 2$)								
1	0.677	0.745	0.677	0.718	0.682	0.638	0.588	0.563
2	0.819	0.902	0.829	0.907	0.819	0.813	0.695	0.672
3	0.791	0.845	0.785	0.825	0.789	0.759	0.742	0.714
4	0.764	0.813	0.769	0.798	0.766	0.762	0.696	0.665
5	0.732	0.806	0.751	0.799	0.796	1.061	0.672	0.637
6	1.407	1.271	0.914	1.272	1.400	1.226	1.142	1.192
7	**0.789**	**1.338**	**0.816**	**1.128**	**0.800**	**0.947**	**0.674**	**0.947**
8	0.791	0.845	0.796	0.837	0.789	0.759	0.742	0.714
9	1.170	1.271	1.125	1.028	1.186	1.226	1.341	1.192
10	0.819	0.902	0.832	0.871	0.819	0.813	0.695	0.672
11	**0.732**	**0.806**	**0.861**	**0.842**	**0.857**	**1.061**	**0.667**	**0.637**
12	0.677	0.745	0.672	0.723	0.682	0.638	0.588	0.563

$$u = r^{2/3} \sin \frac{2\theta}{3} \tag{2.11b}$$

We see that the performance of all estimators is poor in the cells adjoint to the vertex and far from the vertex. The low effectivity index is directly related to the pollution, the strength of which is increasing with the strength of the singularity and degree of elements. Hence, we can conclude that in the neighborhood of the vertex we have to use another error estimator which is of higher quality. This is essential for the a-posteriori error estimation of the pollution inside the domain (see [22]). One of the natural ways is to extract the stress intensity factor and use it in the estimator. For that we need to know the character of the solution (the singular terms). For the Laplace equation this character is simple. For the elasticity equations the singular terms have to be computed numerically (see [23, 24]). We can then easily extract the value of the effectivity index. There are many ways to get them. As an example, we mention the contour integral method (CIM) and *cut-off function method* (CFM) [25, 26], various projection methods (see [27]), *discrete projection method* (DPK) which is analogous to the ZZ estimators, and others. For detailed results, we refer to [28]. Then we construct the estimator as the norm of the difference between recovered solution (using one term of singular expansion with computed stress effectivity index by particular extraction) and the finite element solution.

As an example, we will compute the effectivity index in the ℓth layer of the cells for the chevron pattern.

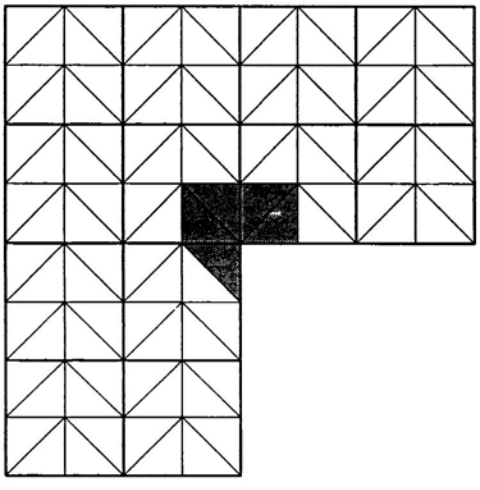

Fig. 2.5. The domain with chevron elements. The first layer is shaded and the second layer is unshaded.

In Table 2.3a we report the effectivity indices for certain layers using the CIM, CFM

and DPK extraction methods for different singularities λ and for $p = 1$. When $p = 2$, we get the results shown in Table 2.3b. Tables 2.3a and 2.3b show that we can get error

Table 2.3a. The layer effectivity index based on the various extraction methods and on the *ERpB* and *ZZ* estimators, for different singularities λ and for $p = 1$.

Extraction Technique	Layer											
	$\lambda = 1/4$			$\lambda = 1/2$			$\lambda = 1/3$			$\lambda = 2/3$		
	1	2	6	1	2	6	1	2	6	1	2	6
CIM	0.94	0.94	0.89	0.99	0.99	0.99	0.98	0.98	0.93	0.99	1.00	1.00
CFM	0.93	0.94	0.89	0.99	0.99	0.98	0.97	0.97	0.93	0.99	1.00	1.00
DPK	0.99	0.98	0.96	1.02	1.03	1.19	1.02	1.02	1.10	1.01	1.01	1.17
ERpB	1.67	0.73	0.33	1.12	0.89	0.81	1.57	0.79	0.48	1.02	0.94	0.96
ZZ	0.75	0.71	0.32	1.07	0.91	0.78	0.74	0.80	0.46	1.03	0.93	0.93

Table 2.3b. The layer effectivity index based on the various extraction methods and on the *ERpB* and *ZZ* estimators, for different singularities λ and for $p = 2$.

Extraction Technique	Layer											
	$\lambda = 1/4$			$\lambda = 1/2$			$\lambda = 1/3$			$\lambda = 2/3$		
	1	2	6	1	2	6	1	2	6	1	2	6
CIM	0.96	0.99	0.88	0.99	1.00	0.97	0.98	1.00	0.92	1.00	1.00	1.04
CFM	0.96	0.99	0.88	0.99	1.00	0.96	0.99	1.00	0.92	1.00	1.00	0.99
DPK	0.89	1.23	1.60	0.99	1.65	7.52	1.04	1.09	1.65	1.05	2.15	21.00
ERpB	1.82	0.36	0.03	1.08	0.69	0.21	1.61	0.43	0.06	0.96	0.84	0.63
ZZ	0.80	0.53	0.04	1.16	0.92	0.22	0.80	0.72	0.06	1.15	1.22	0.65

estimators of high quality but accurate extraction of the effectivity index is necessary, especially for the elements which are not adjoint to the vertex. From Table 2.3 we see that the DPK method leads to poor effectivity index.

2.4 A-posteriori lower and upper estimate of the error in the energy norm on Ω for the classical finite element method

Let us be interested in the energy norm of the error on the entire domain Ω for the problem (1.1). Let us denote by ε_τ the edges of the elements τ and consider the usual equilibrated residual error estimator

$$\eta(\tau) = ||\varphi_\tau||_{\mathcal{U}(\tau)} \tag{2.12}$$

where φ_τ is the solution of the Neumann problem on τ with the residual on the right hand side and boundary conditions obtained by the equilibration (see, e.g., [19] for the definition). Then we have:

Theorem 2.4. We have

$$||e_h||_{\mathcal{U}} \leq \sqrt{\sum_\tau \eta^2(\tau)} = \mathcal{E}(u_h) \tag{2.13}$$

□

Estimate (2.13) holds for any $u_0 \in H^1(\Omega)$ solving (1.1). Function φ_τ which solves the associated Neumann problem is unique up to a constant. Hence we will assume that $\int_\tau \varphi_\tau = 0$. Although we assume that φ_τ is the exact solution, in practice we will solve it approximately, e.g., by the p-version of FEM or by fine mesh on τ.

Estimate (2.13) is obviously the guaranteed *upper* estimate of the error e_h.

Let us now derive the lower estimate of the error and an improved upper one.

Let $\Phi \in L^2(\Omega)$ such that $\Phi|_\tau = \varphi_\tau$. Then Φ is discontinuous over the edges ε_τ of the elements. Let us call the jump on the edge ε_τ the $gap_\Phi(\varepsilon_\tau)$. We will first modify the function φ_τ by adding a bilinear function w_τ on τ so that the gap_Φ of $\Psi = \Phi + W$ vanishes at the nodal points of the mesh, where $W|_\tau = w_\tau$. We note that w_τ is a bilinear function and hence $\Delta w_\tau \equiv 0$ and we have

$$\left.\begin{aligned} \Delta\Psi|_\tau &= \Delta\varphi_\tau \\ \left[\!\left[\frac{\partial\Psi}{\partial n_{\varepsilon_\tau}}\right]\!\right] &= \left[\!\left[\frac{\partial\Phi}{\partial n_{\varepsilon_\tau}}\right]\!\right] + \left[\!\left[\frac{\partial W}{\partial n_{\varepsilon_\tau}}\right]\!\right], \qquad \varepsilon_\tau \subset \partial\tau \end{aligned}\right\} \tag{2.14}$$

where n_{ε_τ} is the normal assigned to the edges and $[\![v]\!]$ denotes the jump in v across the edges. Let $s \in \mathcal{U}(\Omega)$ be the exact solution of

$$\int_\Omega \nabla s \cdot \nabla v = \sum_{\tau \in T_h} \sum_{\varepsilon_\tau \subset \partial\tau} \int_{\varepsilon_\tau} \left[\!\left[\frac{\partial w}{\partial n_{\varepsilon_\tau}}\right]\!\right] v, \qquad \forall\, v \in \mathcal{U}(\Omega) \tag{2.15}$$

and let $s_h \in V^h(\Omega)$ be the corresponding finite element approximation. The solution to (2.15) exists because

$$\sum_{\tau \in T_h} \sum_{\varepsilon_\tau \subset \partial\tau} \int_{\varepsilon_\tau} \left[\!\left[\frac{\partial w}{\partial n_{\varepsilon_\tau}} \right]\!\right] = \sum_{\tau \in T_h} \oint_{\partial\tau} \frac{\partial w}{\partial n} = \sum_{\tau \in T_h} \int_\tau \nabla w \cdot \nabla 1 = 0$$

We remark that the upper bound of the error $s - s_h$ is computable by Theorem 2.4.

Let us now construct $\rho_\tau \in \mathcal{U}(\tau)$ such that it is continuous across inter-element edges, i.e., ρ_τ satisfies the following

$$\left.\begin{array}{rll} \Delta\rho_\tau \equiv & 0 & \text{in } \tau \\ \rho_\tau = \text{sign}(\tau, \tau^*) & \frac{1}{2}\, gap_\Phi(\varepsilon_\tau) & \text{on } \varepsilon_\tau \subset \partial\tau \\ \rho_\tau = & \Psi & \text{on } \Gamma \end{array}\right\} \tag{2.16}$$

where ε_τ is the common edge for two adjacent elements τ and τ^* and $\text{sign}(\tau, \tau^*) = 1$ if $\text{index}(\tau) > \text{index}(\tau *)$; $\text{sign}(\tau, \tau^*) = -1$ if $\text{index}(\tau) < \text{index}(\tau^*)$. Note that the solution to the above Dirichlet problem exists because $gap_\Phi(\varepsilon_\tau) = 0$ on the ends on the edge. Let $R \in L^2(\Omega)$ be such that $R|_\tau = \rho_\tau$ and further let $\zeta \in \mathcal{U}(\Omega)$ be the solution of

$$\int_\Omega \nabla\zeta \cdot \nabla v = \sum_{\tau \in T_h} \int_\tau \nabla\rho_\tau \cdot \nabla v \qquad \forall\, v \in \mathcal{U}(\Omega)$$

By employing Cauchy-Schwarz inequality, we have

$$||\zeta||_{\mathcal{U}(\Omega)} \leq \sqrt{\sum_{\tau \in T_h} ||\rho_\tau||^2_{\mathcal{U}(\tau)}}$$

Let $\Lambda = R - \zeta$ and let

$$\mathcal{U}^*(\Omega) =_{\text{df}} \left\{ u \,\middle|\, u|_\tau \in \mathcal{U}(\tau),\ ||u||_{\mathcal{U}^*(\tau)} =_{\text{df}} \sqrt{\sum_{\tau \in T_h} ||u||^2_{\mathcal{U}(\tau)}} < \infty \right\}$$

and Λ satisfies the following:

1. $\Delta\Lambda \equiv 0$ on τ
2. $gap_\Lambda(\varepsilon_\tau) = gap_\Psi(\varepsilon_\tau)$
3. $\Lambda - R \in C^0(\Omega)$
4. $\left[\!\left[\frac{\partial\Lambda}{\partial n_{\varepsilon_\tau}} \right]\!\right] = 0$ for all ε_τ

5. $\sum_{\tau \in T_h} \int_\tau \nabla \Lambda \cdot \nabla v = 0 \; \forall \; v \in \mathcal{U}(\Omega)$

Therefore we have

$$\sum_{\tau \in T_h} \int_\tau \nabla \Lambda \cdot \nabla (\Lambda - R) = 0 \tag{2.17}$$

and by employing the Cauch-Schwarz inequality we get

$$||\Lambda||_{\mathcal{U}^*(\tau)} \leq ||R||_{\mathcal{U}^*(\tau)} \tag{2.18}$$

which yields computational upper estimate for $||\Lambda||_{\mathcal{U}^*(\Omega)}$. We now have

$$u_0 - u_h = e_h = \Psi - s - \Lambda \tag{2.19a}$$

or

$$\Psi = e_h + s + \Lambda \tag{2.19b}$$

where

$$e_h + s = \Psi - \Lambda \in H^1_{\mathrm{D}}$$

and

$$\sum_{\tau \in T_h} \mathcal{B}_\tau (e_h + s, \Lambda) = 0$$

Hence

$$||\Psi||^2_{\mathcal{U}^*(\Omega)} = ||e_h + s||^2_{\mathcal{U}^*(\Omega)} + ||\Lambda||^2_{\mathcal{U}^*(\Omega)}$$

But

$$e_h + s = e_h + s_h - (s - s_h)$$

and

$$||e_h - s||^2_{\mathcal{U}^*(\Omega)} = ||e + s_h - (s - s_h)||^2_{\mathcal{U}^*(\Omega)} = ||e_h + s_h||^2_{\mathcal{U}^*(\Omega)} + ||s - s_h||^2_{\mathcal{U}^*(\Omega)} - 2 \sum_{\tau \in T_h} \mathcal{B}_\tau (e + s_h, (s - s_h))$$

$$= ||e_h||^2_{\mathcal{U}^*(\Omega)} + ||s_h||^2_{\mathcal{U}^*(\Omega)} + ||s - s_h||^2_{\mathcal{U}^*(\Omega)} - 2 \sum_{\tau \in T_h} \mathcal{B}_\tau (e_h, s - s_h)$$

where we employed the fact that $s_h \in S^p_\Delta$. Hence

$$||\Psi||^2_{\mathcal{U}^*(\Omega)} = ||e_h||^2_{\mathcal{U}^*(\Omega)} + ||s_h||^2_{\mathcal{U}^*(\Omega)} + ||s - s_h||^2_{\mathcal{U}^*(\Omega)} - 2 \sum_{\tau \in T_h} \mathcal{B}_\tau (e_h, s - s_h) + ||\Lambda||^2_{\mathcal{U}^*(\Omega)}$$

or

$$||e_h||^2_{\mathcal{U}(\Omega)} - 2\gamma \, ||e_h||_{\mathcal{U}(\Omega)} \; ||s - s_h||_{\mathcal{U}(\Omega)} = ||\Psi||^2_{\mathcal{U}^*(\Omega)} - ||\Lambda||^2_{\mathcal{U}^*(\Omega)} - ||s_h||^2_{\mathcal{U}(\Omega)} - ||s - s_h||^2_{\mathcal{U}(\Omega)} \tag{2.20}$$

where $|\gamma| \leq 1$. In (2.20) we used the fact that $||e_h||_{\mathcal{U}^*(\Omega)} = ||e||_{\mathcal{U}(\Omega)}$, etc. From (2.18) we get

$$||e_h||_{\mathcal{U}(\Omega)} \leq \mathcal{E}(s_h) + ||\Psi||_{\mathcal{U}^*(\Omega)} = E^U(u_h) \tag{2.21}$$

where we used (2.16) and (2.13) for s_h. (2.21) is guaranteed upper bound of the error (2.20) also yields lower bound. In fact we have

$$||e_h|| \geq -\mathcal{E}(s_h) + \left(||\Psi||^2_{\mathcal{U}^*(\Omega)} - ||R||^2_{\mathcal{U}^*(\Omega)} - ||s_h||^2_{\mathcal{U}^*(\Omega)}\right)^{1/2} = E^L(u_h) \tag{2.22}$$

Estimates (2.21) and (2.22) give the bound on the effectivity index. In fact

$$\frac{\mathcal{E}}{E^U} \leq \kappa(\mathcal{E}) \leq \frac{\mathcal{E}}{E^L}$$

and

$$\kappa(E^U) = \frac{E^U}{||e||} \leq \frac{E^U}{E^L} \qquad \frac{E^L}{||e||} = \kappa(E^L) \geq \frac{E^L}{E^U}$$

The estimate (2.21) is more expensive; nevertheless, not too much expensive because it consists of the computation of s_h for which the LU decomposition of the stiffness matrix of the original problem is used and hence it is only vector multiplication by a sparse matrix. Computation of Ψ, R and $\mathcal{E}(s_h)$ is local. The estimates (2.21) and (2.22) hold for rectangular elements (see example) and much more general assumptions on the elements, e.g., curvilinear ones, the elasticity equations, etc., after certain minor modifications.

Example 2.1. Let us solve the problem (1.1) on $\Omega = (-1,1) \times (-1,1)$ with $\Gamma_D = \emptyset$ and the exact solution

$$u_0 = \sin 4x \ \sinh 4y \tag{2.23}$$

We will consider uniform mesh with square elements of size h and the classical FEM with tensor product elements of degree $p = 2$. In Table 2.4 we report the absolute and relative error, the terms in (2.20) and (2.21), the estimators and the effectivity indices $\kappa(\mathcal{E})$, $\kappa(E^U)$ and $\kappa((E^U + E^L)/2)$. We solved the local problems using polynomial of degree $p = 6$. We note that the upper bound for the energy norm of the error converges to unity asymptotically.

2.5 Upper and lower error estimate for computation of the values of linear functional for the classical finite element method

Often we are not interested in the accuracy of the solution measured in the energy norm or another norm. We are interested in the values of special functional, i.e., in the values

Table 2.4. The upper and lower estimates and the terms in (2.20) and (2.21) for the problem of Example 2.1.

	$h = 1/8$	$h = 1/16$	$h = 1/32$
$\|\|e_h\|\|_{\mathcal{U}}$	0.20156564(+1)	0.6371886(0)	0.15736169(0)
$\|\|e_h\|\|_{\mathcal{U}} / \|\|\mathcal{E}\|\|_{\mathcal{U}}$	4.92%	1.49%	0.368%
$\mathcal{E}(u_h)$	0.2959078(+1)	0.73171422(0)	0.18081334(0)
$\|\|\Psi\|\|_{\mathcal{U}}$	0.20046381(+1)	0.49324324(0)	0.14094857(0)
$\|\|s_h\|\|_{\mathcal{U}}$	0.70613441(0)	0.17470508(0)	0.43539518(-1)
$\mathcal{E}(s_h)$	0.46281394(0)	0.13418581(0)	0.23453608(-1)
$\|\|\Lambda_1\|\|_{\mathcal{U}}$	0.43016872(0)	0.10621730(0)	0.26745704(0)
$E^U(u_h)$	0.26312799(1)	0.66812669(0)	0.17337860(0)
$E^L(u_h)$	0.13633577(1)	0.58305651(0)	0.15481612(0)
$\kappa(\mathcal{E})$	1.468	1.212	1.149
$\kappa(E^U)$	1.305	1.107	1.102
$\kappa((E^U + E^L)/2)$	0.991	1.035	1.043

$e(u_h)$. The functional $e(u_h)$ could be stress intensity factor value; some integrals of u_h over a domain or line (e.g., the boundary), or in the stresses in some point, etc. Here for simplicity we will assume that ℓ is linear functional of $\mathcal{U}(\Omega)$. The error was estimated in [31] and here we will elaborate on it in the light of the estimates (2.13), (2.20) and (2.21). Because ℓ is linear bounded functional on $\mathcal{U}(\Omega)$, there exists $G \in \mathcal{U}(\Omega)$ such that

$$\ell(u) = (G, u)_{\mathcal{U}(\Omega)} \forall u \in \mathcal{U}(\Omega) \tag{2.24}$$

Because $(\cdot, \cdot)_{\mathcal{U}(\Omega)}$ is the scalar product we have

$$\ell(u) = (G, u)_{\mathcal{U}(\Omega)} = \frac{1}{4}\Big(||G + u||^2_{\mathcal{U}(\Omega)} - ||G - u||^2_{\mathcal{U}(\Omega)}\Big)$$

$$\ell(u_h) = (G_h, u_h)_{\mathcal{U}(\Omega)} = \frac{1}{4}\Big(||G_h + u_h||^2_{\mathcal{U}(\Omega)} - ||G_h - u_h||^2_{\mathcal{U}(\Omega)}\Big)$$

Further

$$||G + u||^2_{\mathcal{U}(\Omega)} = ||G_h + u_h||^2_{\mathcal{U}(\Omega)} + ||e_h(G + u)||^2_{\mathcal{U}(\Omega)}$$

$$||G - u||^2_{\mathcal{U}(\Omega)} = ||G_h - u_h||^2_{\mathcal{U}(\Omega)} + ||e_h(G - u)||^2_{\mathcal{U}(\Omega)}$$

where we denoted

$$(G + u) - (G_h + u_h) = e_h(G + u)$$

$$(G-u)-(G_h-u_h)=e_h(G-u)$$

Then we have

$$\begin{aligned}\ell(u)-\ell(u_h) &= \frac{1}{4}\Big(||G+u||^2_{\mathcal{U}(\Omega)}-||G_h+u_h||^2_{\mathcal{U}(\Omega)}-\big(||G-u||^2_{\mathcal{U}(\Omega)}-||G_h-u_h||^2_{\mathcal{U}(\Omega)}\big)\Big)\\ &= \frac{1}{4}\Big(||e_h(G+u)||^2_{\mathcal{U}(\Omega)}-||e_h(G-u)||^2_{\mathcal{U}(\Omega)}\Big)\end{aligned} \tag{2.25}$$

Hence using (2.13) we get

$$\ell(u)-\ell(u_h)\le\frac{1}{4}\Big(\mathcal{E}^2(G_h+u_h)\Big) \tag{2.26a}$$

$$\ell(u)-\ell(u_h)\ge-\frac{1}{4}\Big(\mathcal{E}^2(G_h-u_h)\Big) \tag{2.26b}$$

Using (2.20) and (2.21) we get better estimate

$$\ell(u)-\ell(u_h)\le\frac{1}{4}\Big(\big(E^U(G_h+u_h)\big)^2-\big(E^L(G_h-u_h)\big)^2\Big) \tag{2.27a}$$

$$\ell(u)-\ell(u_h)\ge-\frac{1}{4}\Big(\big(E^U(G_h-u_h)\big)^2-\big(E^L(G_h+u_h)\big)^2\Big) \tag{2.27b}$$

and hence

$$|\ell(u)-\ell(u_h)|\le\frac{1}{4}\max\Big(\mathcal{E}^2(G_h+u_h),\mathcal{E}^2(G_h-u_h)\Big) \tag{2.28a}$$

or

$$|\ell(u)-\ell(u_h)|\le\max\frac{1}{4}\Big(\big(E^U(G_h+u_h)\big)^2-\big(E^L(G_h-u_h)\big)^2,\big(E^U(G_h-u_h)\big)^2-\big(E^L(G_h+u_h)\big)^2\Big) \tag{2.28b}$$

(2.28a) leads to an adaptive procedure when the mesh is designed for simultaneous cases (G_h+u_h) and (G_h-u_h) and for the final error estimate we are using either (2.27) or (2.28b).

Although the estimates (2.28a) as guaranteed estimates is valid only for the equilibrated residual estimator, it can be used for the other estimators too.

Example 2.2. Let us consider once more the problem of the Example 2.1 and let us be interested in the value of the functional

$$\ell(u)=\int_{-1}^{+1}u(1,y)\,\sin y \tag{2.29}$$

In the Table 2.5 we report the same values as in Table 2.4 for functions $(u+G)$ and $(u-G)$ and in Table 2.6 we report the estimates of the error given by (2.26), (2.27) and (2.28).

Table 2.6. The estimation of the upper and lower bounds for the quantity of interest (2.29) by employing (2.28).

Estimation of error in the quantity of interest		
$h = 1/8$, Exact error = 0.3119655252		
	$u+G$	$u-G$
$\|\|\Psi\|\| =$	1.2130478621	0.5519948006
$\|\|s_h\|\| =$	0.7358120869	0.3284172961
$\|\|\mathcal{E}(s_h)\|\| =$	0.4682668318	0.1974621762
$\|\|R\|\|_{\mathcal{U}^*(\Omega)} =$	0.2024562508	0.1036622226
$E^U =$	1.681314707	0.7494570017
$E^L =$	0.4746420383	0.2339245230
Upper Bound = $0.6930246353 \times 10^{0}$ Lower Bound = $-0.8410018682 \times 10^{-1}$		
$h = 1/16$, Exact error= $0.1949784532 \times 10^{-1}$		
	$u+G$	$u-G$
$\|\|\Psi\|\| =$	0.3040674031	0.1383652091
$\|\|s_h\|\| =$	0.1836807915	$0.8201689121 \times 10^{-1}$
$\|\|\mathcal{E}(s_h)\|\| =$	$0.5902187966 \times 10^{-1}$	$0.2551351304 \times 10^{-1}$
$\|\|R\|\|_{\mathcal{U}^*(\Omega)} =$	$0.5060230568 \times 10^{-1}$	$0.2590953372 \times 10^{-1}$
$E^U =$	0.3630892932	0.1638787240
$E^L =$	0.1779544055	$0.8286940306 \times 10^{-1}$
Upper Bound = $0.3124162368 \times 10^{-1}$ Lower Bound = $0.1202883548 \times 10^{-2}$		
$h = 1/32$, Exact error= $0.1218615333 \times 10^{-2}$		
	$u+G$	$u-G$
$\|\|\Psi\|\| =$	$0.6821126491 \times 10^{-1}$	$0.3125644475 \times 10^{-1}$
$\|\|s_h\|\| =$	$0.4587138677 \times 10^{-1}$	$0.2050261946 \times 10^{-1}$
$\|\|\mathcal{E}(s_h)\|\| =$	$0.7301681275 \times 10^{-2}$	$0.3084401629 \times 10^{-2}$
$\|\|R\|\|_{\mathcal{U}^*(\Omega)} =$	$0.1007128041 \times 10^{-1}$	$0.4696347751 \times 10^{-2}$
$E^U =$	$0.7551294565 \times 10^{-1}$	$0.3434084728 \times 10^{-1}$
$E^L =$	$0.4216711596 \times 10^{-1}$	$0.2003598399 \times 10^{-1}$
Upper Bound = $0.1325191115 \times 10^{-2}$ Lower Bound = $0.1496929617 \times 10^{-3}$		

2.6 A-posteriori error estimation for the generalized finite element method

As we have seen in Section 1 $S^1_\Delta \subset S_\Delta(\Psi)$ and hence the equilibrated residual estimate can be used here too, but without, in general, the usual higher order equilibration. Hence Theorem 2.4 and the estimate (2.13) hold too. The asymptotic analysis parallel to the Theorems 2.1–2.3 as well as the superconvergence analysis can be made here for the GFEM too. The recovery error estimations which are based directly or indirectly on the superconvergence could loose its effectiveness. On the other hand, the recovery error estimate based on the least-squares approximation are valid for the GFEM too.

Example 2.3. Let us solve the same problem as in Example 2.1 using the classical FE method with tensor product elements of degree $p = 2$ and GFEM with Ψ consisting of linear functions. In Table 2.7 we report the effectivity index of the equilibrated (with linear equilibration) residual estimate when the associated Neumann problem is solved using polynomials of degree 3. Further, we report the effectivity index based on the least-squares patch recovery with harmonic functions of degree 3.

Table 2.7. The effectivity index of FEM and GFEM for the residual and least-squares recovery. Exact solution $u_0 = \sin 4x \, \sinh 4y$.

	Residual Estimate		Least-squares Recovery Estimate	
h	FEM	GFEM	FEM	GFEM
1	0.96843	1.05298	2.58026	1.23889
1/2	1.14646	1.09917	3.33831	2.88947
1/4	1.21211	1.20036	2.70627	2.59246
1/8	1.10966	1.10832	1.58466	1.56577
1/16	1.03809	1.03797	1.10360	1.09932
1/32	1.01112	1.01105	1.00900	1.00791

Remark If the associated Neumann problem would be solved locally, then for the residual estimate we have $\kappa \geq 1$. The approximate solution underestimates the error, as can be seen from the Table for $h = 1$.

From the Table we see that both estimates, the residual and the least squares, are of the same quality. The lower and upper estimate given in the Section 2.5 holds here too

because $S^1_\Delta \subset S_\Delta(\Psi)$. The same is true for the lower and upper estimates for the error in the linear functional; nevertheless, if the function G cannot be well approximated by $S_\Delta(\Psi)$ (although u_0 could), then the accuracy of the linear functional will be poor.

Acknowledgments

The work of I. B. was supported by the Office of Naval Research under contracts N00014-90-J-1030 and N00014-96-10019, and by the National Science Foundation under Grant DMS-91-20877. The work of T.S. and S.K.G. was supported by the U.S. Army Research Office under Grant DAAL03-G-028, by the National Science Foundation under Grant MSS-9025110 and by the Office of Naval Research under Grant N00014-96-1-0021 and Grant N00014-96-1-1015.

References

[1] Babuška, I., Caloz, G. and Osborn, J., 'Special finite element methods in a class of second order elliptic problems with rough coefficients,' *SIAM Num. Anal.*, **31**, 945–981 (1994).

[2] I. Babuška and J.M. Melenk, 'The Partition of Unity Method,' *Int. J. Numer. Methods Engrg.*, **40**, 727–758 (1997).

[3] Melenk, J.M. and Babuška, I., 'The partition of unity finite element method: Basic theory and applications,' *Comp. Meth. Appl. Mech. Engrg.*, **139**, 289–314 (1996).

[4] Melenk, J.M. , 'On generalized finite element methods,' Ph.D. Thesis, University of Maryland, College Park, (1995), (Advisor: I. Babuška).

[5] C.A. Duarte, J.T. Oden, '*Pp* Clouds – An *hp* Meshless Method,' *Numer. Meth. for Partial Diff. Eqns.*, **12**, 673–705 (1996).

[6] I.S. Duff and J.K. Reid, 'The multifrontal solution of indefinite sparse symmetric linear systems,' *ACM Trans. Math. Softw.*, **9**, 302–325 (1983).

[7] I.S. Duff and J.K. Reid, 'MA27 – A set of FORTRAN subroutines for solving sparse symmetric sets of linear equations,' *AERE R10533*, HMSO, London (1982).

[8] J. Berntson, T.O. Espelid and A. Genz, 'An adaptive algorithm for the approximate calculation of multiple integrals,' *ACM Trans. Math. Softw.*, **17**, 437–451 (1991).

[9] T.O. Espelid, 'On integrating vertex singularities using extrapolation,' *BIT*, **34**, 62–79 (1994).

[10] J.T. Oden and C.A.M. Duarte, 'Solution of singular problems using *hp* clouds' in *The Mathematics of Finite Elements and Applications*, J.R. Whiteman, ed., John Wiley, 35–54 (1997).

[11] J.T. Oden, C.A.M. Duarte and O.C. Zienkiewicz, 'A New Cloud Based *hp* Finite Element Method,' *Int. J. Numer. Methods Engrg.*, (1997) (to appear).

[12] J. Jirousek and A. Wrobleski, 'T-elements: State of the art and future trends', *Archives of Computational Methods in Engineering, State of Art Reviews*, **3**, 323–435 (1996).

[13] T. Belytschko, Y. Krongauz, D. Organ, M. Fleming and P. Krysl, 'Meshless methods: An overview and recent developments', *Comp. Meth. Appl. Mech. Engrg.*, **139**, 3–48 (1996).

[14] A. Duarte, 'A review of some meshless methods to solve partial differential equations,' *Tech. Rep. TICAM 95-06*, University of Texas at Austin.

[15] I. Babuška, T. Strouboulis, C.S. Upadhyay and S.K. Gangaraj, 'Computer-based proof of the existence of superconvergence points in the finite element method. Superconvergence of the derivatives in finite element solutions of Laplace's, Poisson's and the elasticity equations', *Numer. Methods for PDEs*, **12**, 347–392 (1996).

[16] I. Babuška, T. Strouboulis, S.K. Gangaraj, K. Copps and D.K. Datta, A-posteriori estimation of the error in the error estimate, (this proceeding).

[17] I. Babuška, T. Strouboulis and C.S. Upadhyay, 'A model study of the quality of a-posteriori error estimators for linear elliptic problems. Error estimation in the interior of patchwise uniform grids of triangles', *Comput. Methods Appl. Mech. Engrg.*, **114**, 307–378 (1994).

[18] I. Babuška, T. Strouboulis, C.S. Upadhyay and S.K. Gangaraj and K. Copps, 'An Objective Criterion for Assessing the Reliability of A-posteriori Error Estimators in Finite Element Computations,' *USACM Bulletin*, **7**, 4–15 (1994) and *IACM Bulletin*, **9**, 27–37 (1994).

[19] I. Babuška, T. Strouboulis, C.S. Upadhyay and S.K. Gangaraj and K. Copps, 'Validation of a posteriori error estimators by numerical approach', *Internat. J. Numer. Methods Engrg.*, **37**, 1073–1123 (1994).

[20] I. Babuška, T. Strouboulis and C.S. Upadhyay, 'A model study of the quality of a-posteriori error estimators for finite element solutions of linear elliptic problems with particular reference to the behavior near the boundary', *Int. J. Numer. Methods Engrg.*, **40**, 2521–2577 (1997).

[21] I. Babuška, T. Strouboulis and C.S. Upadhyay, 'Analysis of the local quality of a-posteriori error estimators near a vertex', (to appear).

[22] I. Babuška, T. Strouboulis, A. Mathur and C.S. Upadhyay, Pollution-error in the h-version of the finite-element method and the local quality of a-posteriori error estimators, *Finite Elements in Analysis and Design*, **17**, 237–321 (1994).

[23] P.J. Papadakis and I. Babuška, 'A numerical procedure for the determination of certain quantities related to the stress intensity factors in two-dimensional elasticity,' *Comp. Meth. Appl. Mech. Engrg.*, **122**, 69–92 (1995).

[24] D. Vasilopoulos, 'On the determination of higher order terms of singular elastic stress fields near corners,' *Num. Math.*, **53**, 51–98 (1988).

[25] B.A. Szabo and I. Babuška, *Finite Element Analysis*, John Wiley & Sons, Inc., New York, 1991.

[26] I. Babuška and A. Miller, 'The post-processing approach in the finite element method, Part 2: The calculation of stress intensity factors,' *Int. J. Numer. Methods Engrg.*, **20**, 1111–1129 (1984).

[27] L.B. Wahlbin, Local behavior in finite element methods, in: P.G. Ciarlet and J.L. Lions, eds., *Handbook of Numerical Analysis, Vol. II*, Finite Element Methods Part 1, (North-Holland, Amsterdam, 1991) 357–522.

[28] I. Babuška, T. Strouboulis and C.S. Upadhyay, 'Improved error estimators for mesh patches near the vertex', (to appear).

[29] I. Babuška and W. C. Rheinboldt, 'Error estimates for adaptive finite element computations', *SIAM J. Numer. Anal.*, **15**, 736-754 (1978).

[30] I. Babuška and A. Miller, A feedback finite element method with a-posteriori error estimation,' *Comp. Meth. Appl. Mech. Engrg.*, **61**, 1–40 (1987).

[31] I. Babuška and A. Miller, 'The post-processing approach in the finite element method, Part 3: A-posteriori error estimates and adaptive mesh selection ,' *Int. J. Numer. Methods Engrg.*, **20**, 2311–2324 (1984).